Why Are Proton Transfers at Carbon Slow?
Self-Exchange Reactions

Cyrille Costentin and Jean-Michel Savéant

*Contribution from the Laboratoire d'Electrochimie Moléculaire, Unité Mixte de Recherche
Université, CNRS No. 7591, Université de Paris 7, Denis Diderot, 2 place Jussieu,
75251 Paris Cedex 05, France*

Received June 15, 2004; E-mail: saveant@paris7.jussieu.fr

Abstract: When the quantum character of proton transfer is taken into account, the intrinsic slowness of self-exchange proton transfer at carbon appears as a result of its nonadiabatic character as opposed to the adiabatic character of proton transfer at oxygen and nitrogen. This difference is caused by the lesser polarity of C−H bonds as compared to that of O−H and N−H bonds. Besides solvent and heavy-atom intramolecular reorganizations, the kinetics of the reaction are consequently governed at the level of a pre-exponential term by proton tunneling through the barrier. These contrasting behaviors are illustrated by an analysis of the $CH_3H + {}^-CH_3$, $H_2O + OH^-$, and ${}^+NH_4 + NH_3$ self-exchange reactions. The effect of electron-withdrawing substituents and the case of cation radicals are discussed within the same framework taking the $O_2NCH_2H + CH_2{=}NO_2^-$ and ${}^{+\bullet}H_2NCH_2H + {}^\bullet CH_2NH_2$ as examples. Illustrated by the $CH_2{=}CH{-}CH_2H + {}^-CH_2{-}CH{=}CH_2$ couple, it is shown that the "imbalanced character of the transition state" is related to heavy-atom intramolecular reorganization. Combination of these various effects is finally analyzed, taking the $O_2N{-}CH_2{=}CH{-}CH_2H + CH_2{=}CH{-}CH{=}NO_2^-$ and ${}^{+\bullet}H_2N{-}CH_2{=}CH{-}CH_2H + {}^\bullet CH_2{-}CH{=}CH_2{-}NH_2$ couples as examples.

Introduction

Proton transfer at carbon atoms has attracted and continues to attract considerable attention, mostly motivated by attempts to explain the reasons why it appears intrinsically slow, slower than with "normal" (Eigen) acid−base couples, typically involving atoms such as oxygen and nitrogen.[1,2]

A first, difficulty encountered in the deciphering of the reasons that underlie this intrinsic slowness is the fact that, until recently, the experimental data on which the discussions were based concerned two families of rather peculiar acid−base couples. One of these is constituted by carbon acids that bear an electron-withdrawing group directly attached to the carbon atom or is located in a conjugated position to it on unsaturated substituents, such as ketones or nitroalkanes.[1,3−6]

The presence of these substituents makes these acids strong enough to render the experimental determination of the depro-
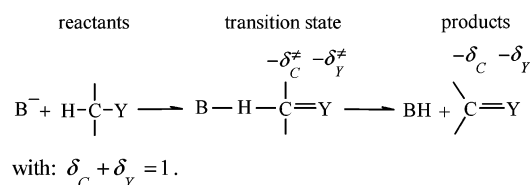
tonation rates by usual bases. The logarithm of the rate constant at zero driving force for these acids ranges from −2 to 5, making their investigation by use of standard methods, such as stopped-flow techniques, achievable.

Another way of making a carbon acid strong enough to be amenable to measuring the deprotonation rate constant is to remove one electron from the molecule. The cation radicals thus generated are indeed much stronger acids than their closed-shell counterparts. Deprotonation of several cation radicals has

(1) For reviews, see: (a) Bernasconi, C. F. *Acc. Chem. Res.* **1987**, *20*, 301. (b) Bernasconi, C. F. *Adv. Phys. Org. Chem.* **1992**, *27*, 119. (c) Bernasconi, C. F. *Acc. Chem. Res.* **1992**, *25*, 9. (d) Bernasconi, C. F.; Ali, M.; Gunter, J. C. *J. Am. Chem. Soc.* **2003**, *125*, 151. (e) Scheiner, S. *Acc. Chem. Res.* **1985**, *18*, 174.

(2) Anne, A.; Fraoua, S.; Hapiot, P.; Moiroux, J.; Savéant, J.-M. *J. Am. Chem. Soc.* **1998**, *120*, 2951 and references therein.

(3) (a) Fukuyama, M.; Flanagan, P. W. K.; Williams, F. T.; Frainer, L.; Miller, S. A.; Schechter, H. *J. Am. Chem. Soc.* **1970**, *92*, 4689. (b) Bordwell, F. G.; Boyle, W. J., Jr. *J. Am. Chem. Soc.* **1972**, *94*, 3907. (c) Bordwell, F. G.; Bartmess, J. E.; Hautala, J. A. *J. Org. Chem.* **1978**, *43*, 3107. (d) Kresge, A. J. *Can. J. Chem.* **1975**, *52*, 1897. (e) Keeffe, J. R.; Munderloh, N. H. *J. Chem. Soc., Chem. Commun.* **1974**, 17. (f) Keeffe, J. R.; Morey, J.; Palmer, C. A.; Lee, J. *J. Am. Chem. Soc.* **1979**, *101*, 1295. (g) Cox, B. G.; Gibson, A. J. *Chem. Soc., Chem. Commun.* **1974**, 638. (h) Wilson, J. C.; Källsson, I.; Saunders, W. H., Jr. *J. Am. Chem. Soc.* **1980**, *102*, 4780. (i) Amin, M.; Saunders, W. H., Jr. *J. Phys. Org. Chem.* **1993**, *6*, 393. (j) Wilson, J. C.; Källsson, I.; Saunders, W. H., Jr. *J. Am. Chem. Soc.* **1980**, *102*, 4780. (k) Amin, M.; Saunders, W. H., Jr. *J. Phys. Org. Chem.* **1993**, *6*, 393.

(4) (a) Bernasconi, C. F.; Kliner, D. A. V.; Mullin, A. S.; Ni, J.-X. *J. Org. Chem.* **1988**, *53*, 3342. (b) Albery, W. J.; Bernasconi, C. F.; Kresge, A. J. *J. Phys. Org. Chem.* **1988**, *1*, 29. (c) Gandler, J. R.; Bernasconi, C. F. *J. Am. Chem. Soc.* **1992**, *114*, 631. (d) Bernasconi, C. F.; Wiersema, D.; Stronach, M. W. *J. Org. Chem.* **1993**, *58*, 217. (e) Bernasconi, C. F.; Ni, J.-X. *J. Org. Chem.* **1994**, *59*, 4910. (f) Bernasconi, C. F.; Panda, M.; Stronach, M. W. *J. Am. Chem. Soc.* **1995**, *117*, 9206. (g) Bernasconi, C. F.; Montanez, R. L. *J. Org. Chem.* **1997**, *62*, 8162. (h) Bernasconi, C. F.; Kittredge, K. W. *J. Org. Chem.* **1998**, *63*, 1994. (i) Bernasconi, C. F.; Wenzel, P. J.; Keeffe, J. R.; Gronert, S. *J. Am. Chem. Soc.* **1997**, *119*, 4008.

(5) (a) Farrell, P. G.; Fogel, P.; Chatrousse, A. P.; Lelièvre, J.; Terrier, F. *J. Chem. Soc., Perkin Trans. 2* **1985**, 51. (b) Fogel, P.; Farrell, P. G.; Lelièvre, J.; Chatrousse, A. P.; Terrier, F. *J. Chem. Soc., Perkin Trans. 2* **1985**, 711. (c) Terrier, F.; Lelièvre, J.; Chatrousse, A. P.; Farrell, P. G. *J. Chem. Soc., Perkin Trans. 2* **1985**, 1479. (d) Lelièvre, J.; Farrell, P. G.; Terrier, F. *J. Chem. Soc., Perkin Trans. 2* **1986**, 333. (e) Farrell, P. G.; Terrier, F.; Xie, H. Q.; Boubaker, T. *J. Org. Chem.* **1990**, *55*, 2546. (f) Terrier, F.; Xie, H. Q.; Farrell, P. G. *J. Org. Chem.* **1990**, *55*, 2610. (g) Terrier, F.; Xie, H. Q.; Lelièvre, J.; Boubaker, T.; Farrell, P. G. *J. Chem. Soc., Perkin Trans. 2* **1990**, 1899. (h) Terrier, F.; Croisat, D.; Chatrousse, A. P.; Ponet, M. J.; Hallé, J. C.; Jacob, G. *J. Org. Chem.* **1992**, *57*, 3684. (i) Terrier, F.; Lan, X.; Farrell, P. G.; Moskowitz, D. *J. Chem. Soc., Perkin Trans. 2* **1992**, 1259. (j) Terrier, F.; Boubaker, T.; Xia, L.; Farrell, P. G. *J. Org. Chem.* **1992**, *57*, 3924. (k) Moutiers, G.; El Fahid, B.; Collot, A.-G.; Terrier, F. *J. Chem. Soc., Perkin Trans. 2* **1996**, 49. (l) Moutiers, G.; Thuet, V.; Terrier, F. *J. Chem. Soc., Perkin Trans. 2* **1997**, 1479. (m) Moutiers, G.; Reignieux, A.; Terrier, F. *J. Chem. Soc., Perkin Trans. 2* **1998**, 2489.

(6) (a) Bednar, R. A.; Jencks, W. P. *J. Am. Chem. Soc.* **1985**, *107*, 7117. (b) Washabaugh, M. W.; Jencks, W. P. *J. Am. Chem. Soc.* **1989**, *111*, 674. (c) Washabaugh, M. W.; Jencks, W. P. *J. Am. Chem. Soc.* **1989**, *111*, 683.

Scheme 1

$$B^- + H\underset{|}{\overset{|}{C}}-Y \longrightarrow B\cdots H\cdots \overset{-\delta_C^{\neq}\ -\delta_Y^{\neq}}{\overset{|}{C}=Y} \longrightarrow BH + \overset{-\delta_C\ -\delta_Y}{\underset{/}{\overset{\backslash}{C}}=Y}$$

reactants   transition state   products

with: $\delta_C + \delta_Y = 1$.

accordingly been investigated by methods ranging from conventional monitoring of concentrations[7] to direct and indirect electrochemistry,[8] pulse radiolysis,[9] and flash photolysis.[8i−k,10] Recently, the laser-flash electron photoinjection method has been applied to the determination of the protonation rate constants of a carbanion bearing no withdrawing substituents, namely, the diphenylmethyl anion, by a series of normal acids.[11]

One consequence of the presence of an electron-withdrawing group directly attached to the functional carbon, or located in a conjugated position to it on an unsaturated substituent, in most of the investigated systems has been the focus of attention to one cause of slowness, which was thought of as a lack of synchronization between the breaking of the carbon−hydrogen bond and delocalization of the charge, at the expense of other possible factors. The result of charge delocalization lagging behind bond breaking would then be an imbalanced transition state, as sketched in Scheme 1.[1a−d]

The imbalanced character of the transition state is defined according to the distribution of charge over the functional carbon and the adjacent group, Y, as shown in the Scheme, with the imbalance expressed as

$$\frac{\delta_C^{\ddagger}}{\delta_Y^{\ddagger}} > \frac{\delta_C}{\delta_Y}$$

for example, the negative charge over the Y group in the transition state is less resonance delocalized than it is in the product state.

Many quantum chemical calculations neglecting the quantum character of proton transfer have been carried out to characterize the transition state of such reactions in the gas phase.[12−16] Most of them have confirmed the intuitive notion that the distribution of charge is not the same in the transition state and in the products.[12,13]

According to these analyses, imbalance of bond breaking and charge delocalization results in an increase of the proton-transfer barrier. With such acids, it is thus difficult to separate the role of nonperfect synchronization from what could be an intrinsic

slowness of carbon acids as opposed to normal acids. The same is true for unsaturated cation radicals. Although less likely, a similar phenomenon is also possible in the case of diphenyl-methane insofar as the charge may be delocalized over the phenyl rings in the carbanion.[11]

There is, however, an even more fundamental problem in analyzing these various factors based on the sole consideration of transition states and activation barriers, such as those derived from the above-mentioned qualitative analyses, models, and quantum chemical calculations. With a proton being a light particle, its transfer cannot be gauged simply in terms of thermal excitation semiclassically overcoming an activation barrier. In other words, quantum effects, notably, the degree of adiabaticity and tunneling from discrete vibrational states, should imperatively be taken into account.[17−19] With a self-exchange reaction, the transition state is only governed by the movement of the heavy particles. Depiction of the reaction coordinate requires considering the effect of the distance, Q, between the two-proton-exchanging centers as well as the intramolecular and solvent reorganizations that occur upon proton transfer, but not the distance, q, defining the location of the proton:

Scheme 2

$$\begin{array}{c}\longleftarrow Q \longrightarrow\\ A \underline{\quad\quad} H \underline{\quad\quad} B^-\\ \leftarrow q \rightarrow\end{array}$$
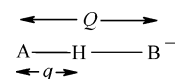
Similar notions have been developed in the analysis of proton transfer taking place along pre-existing H bonds where the role of the Q distance is emphasized, although not fully analyzed in kinetic terms,[20] while Hynes' approach[17] is directly applicable to our purpose of describing the dynamics of proton transfer at carbon. The case where the zero-point energy of the AH, A$^-$ system stands above the proton barrier is called adiabatic. The

(7) (a) Sinha, A.; Bruice, T. C. *J. Am. Chem. Soc.* **1984**, *106*, 7291. (b) Tolbert, L. M.; Khanna, R. K. *J. Am. Chem. Soc.* **1987**, *109*, 3477. (c) Tolbert, L. M.; Khanna, R. K.; Popp, A. E.; Gelbaum, L.; Bettomley, L. A. *J. Am. Chem. Soc.* **1990**, *112*, 2373. (d) Fukuzumi, S.; Kondo, Y.; Tanaka, T. *J. Chem. Soc., Perkin Trans. 2* **1984**, 673. (e) Fukuzumi, S.; Tokuda, Y.; Kitano, T.; Okamoto, T.; Otera, J. *J. Am. Chem. Soc.* **1993**, *115*, 8960.
(8) (a) Schlesener, C. J.; Amatore, C.; Kochi, J. K. *J. Am. Chem. Soc.* **1984**, *106*, 7472. (b) Schlesener, C. J.; Amatore, C.; Kochi, J. K. *J. Phys. Chem.* **1986**, *90*, 3747. (c) Masnovi, J. M.; Sankararaman, S.; Kochi, J. K. *J. Am. Chem. Soc.* **1989**, *111*, 2263. (d) Sankararaman, S.; Perrier, S.; Kochi, J. K. *J. Am. Chem. Soc.* **1989**, *111*, 6448. (e) Reitstöen, B.; Parker, V. D. *J. Am. Chem. Soc.* **1990**, *112*, 4698. (f) Parker, V. D.; Chao, Y.; Reitstöen, B. *J. Am. Chem. Soc.* **1991**, *113*, 2336. (g) Parker, V. D.; Tilset, M. *J. Am. Chem. Soc.* **1991**, *113*, 8778. (h) Hapiot, P.; Moiroux, J.; Savéant, J.-M. *J. Am. Chem. Soc.* **1990**, *112*, 1337. (i) Anne, A.; Hapiot, P.; Moiroux, J.; Neta, P.; Savéant, J.-M. *J. Phys. Chem.* **1991**, *95*, 2370. (j) Anne, A.; Hapiot, P.; Moiroux, J.; Neta, P.; Savéant, J.-M. *J. Am. Chem. Soc.* **1992**, *114*, 4694. (k) Anne, A.; Fraoua, S.; Hapiot, P.; Moiroux, J.; Savéant, J.-M. *J. Am. Chem. Soc.* **1995**, *117*, 7412.
(9) Baciocchi, E.; Bietti, M.; Putignani, L.; Steenken, S. *J. Am. Chem. Soc.* **1996**, *118*, 5952.
(10) (a) Baciocchi, E.; Del Giacco, T.; Elisei, F. *J. Am. Chem. Soc.* **1993**, *115*, 12290. (b) Xu, W.; Mariano, P. S. *J. Am. Chem. Soc.* **1991**, *113*, 1431. (c) Peters, K. S.; Cashin, G. *J. Am. Chem. Soc.* **2000**, *122*, 107. (d) Peters, K. S.; Cashin, G.; Timber, P. *J. Phys. Chem. A* **2000**, *104*, 4833. (e) Peters, K. S.; Kim, G. *J. Phys. Chem. A* **2001**, *105*, 4177. (f) Peters, K. S.; Kim, G. *J. Phys. Chem. A* **2004**, *108*, 2598.
(11) Andrieux, C. P.; Hapiot, P.; Gamby, J.; Savéant, J.-M. *J. Am. Chem. Soc.* **2003**, *125*, 10119.
(12) (a) Bernasconi, C. F.; Wenzel, P. J. *J. Am. Chem. Soc.* **1994**, *116*, 5405. (b) Bernasconi, C. F.; Wenzel, P. J. *J. Am. Chem. Soc.* **1996**, *118*, 10494. (c) Bernasconi, C. F.; Wenzel, P. J. *J. Am. Chem. Soc.* **1996**, *118*, 11446. (d) Bernasconi, C. F.; Wenzel, P. J. *J. Org. Chem.* **2001**, *66*, 968. (e) Bernasconi, C. F.; Wenzel, P. J. *J. Am. Chem. Soc.* **2001**, *123*, 7146.
(13) (a) Saunders, W. J., Jr. *J. Am. Chem. Soc.* **1994**, *116*, 5400. (b) Saunders, W. H., Jr.; Van Verth, J. E. *J. Org. Chem.* **1995**, *60*, 3452. (c) Van Verth, J. E.; Saunders, W. H., Jr. *J. Org. Chem.* **1997**, *62*, 5743. (d) Van Verth, J. E.; Saunders, W. J., Jr. *Can. J. Chem.* **1999**, *77*, 810. (e) Harris, N.; Wei, W.; Saunders, W. H., Jr.; Shaik, S. S. *J. Phys. Org. Chem.* **1999**, *12*, 259. (f) Harris, N.; Wei, W.; Saunders, W. H., Jr.; Shaik, S. *J. Am. Chem. Soc.* **2000**, *122*, 6754.
(14) (a) Gronert, S. *J. Am. Chem. Soc.* **1993**, *115*, 10258. (b) Keefe, J. R.; Gronert, S.; Colvin, M. E.; Tran, N. L. *J. Am. Chem. Soc.* **2003**, *125*, 11730.
(15) Cybulski, S. M.; Scheiner, S. *J. Am. Chem. Soc.* **1987**, *109*, 4199.
(16) (a) McKee, M. L. *J. Am. Chem. Soc.* **1987**, *109*, 559. (b) Wolfe, S.; Hoz, S.; Kim, C.-K.; Yang, K. *J. Am. Chem. Soc.* **1990**, *112*, 4186. (c) Beksic, D.; Bertran, J.; Lluch, J. M.; Hynes, J. T. *J. Phys. Chem. A* **1998**, *102*, 3977. (d) Yamataka, H.; Mustanir; Mishima, M. *J. Am. Chem. Soc.* **1999**, *121*, 10223. (e) Perakyla, M. *J. Chem. Soc., Perkin Trans. 2* **1997**, 2185. (f) Agaback, M.; Lunell, S.; Hussenius, A.; Matsson, O. *Acta Chem. Scand.* **1998**, *52*, 541.
(17) Borgis, D.; Hynes, J. T. *J. Phys. Chem.* **1996**, *100*, 1118.
(18) (a) Babamov, V. K.; Marcus, R. A. *J. Chem. Phys.* **1981**, *74*, 1790. (b) Babamov, V. K.; Lopez, V.; Marcus, R. A. *Chem. Phys. Lett.* **1983**, *101*, 507. (c) Babamov, V. K.; Lopez, V.; Marcus, R. A. *J. Chem. Phys.* **1983**, *78*, 5621. (d) Marcus, R. A. *Faraday Discuss. Chem. Soc.* **1982**, *74*, 7.
(19) Scheiner, S.; Latajka, Z. *J. Phys. Chem.* **1987**, *91*, 724.
(20) (a) Scheiner, S.; Kar, T. *J. Am. Chem. Soc.* **1995**, *117*, 6970. (b) Cleland, W. W. *Biochemistry* **1992**, *31*, 317. (c) Chen, J.; McAllister, M. A.; Lee, J. K.; Houk, K. N. *J. Org. Chem.* **1998**, *63*, 4611.
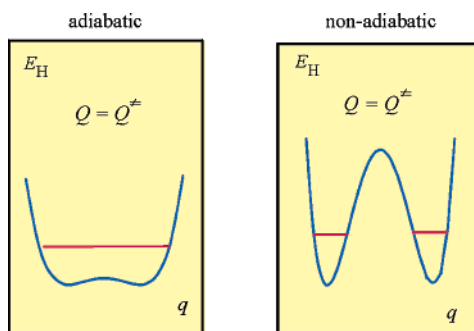
Figure 1. AH, A⁻ self-exchange reaction. Proton potential energy as a function of the A−H distance for an A−A distance corresponding to the transition state in the adiabatic and nonadiabatic case.

dynamics of the reaction is then entirely governed by heavy-atom reorganization. When the zero-point energy lies below the proton barrier, one or a limited number of vibrational states is then involved in proton tunneling through the barrier. This case is called nonadiabatic. The characteristics of the proton barrier will then govern a pre-exponential protonic factor in front of the exponential term, reflecting heavy-atom reorganization. It follows that previous quantum chemical investigations based on the implicit assumption that the rate constant is related to the calculated barrier according to the conventional transition-state theory should be re-examined within this framework. Figure 1 depicts schematically an adiabatic and a nonadiabatic situation in which $Q = Q^{\ddagger}$ shows that the transition state is only governed by the movement of the heavy particles.

Within this context, our strategy was to successively address the main questions raised by the slowness of proton transfer at carbon with the help, in each case, of an illustrating example of the self-exchange reaction. We limit ourselves, here, to the self-exchange reaction because it goes to the nitty-gritty of the problem. Mixed reactions involving a carbon acid and a normal base or vice versa are obviously interesting; particularly interesting is the question of what is the result of combining the nonadiabaticity of the carbon species with the adiabaticity of the normal partner, but they are not relevant to the question of intrinsic slowness. In this connection, the case of proton transfer from HCN is striking; it appears slow when opposed to a cyanide ion and fast when opposed to an oxygen base.[6a] Thus, the first problem we will discuss is that of the intrinsic slowness of proton transfer at carbon. What is the cause of this intrinsic slowness compared to normal acids? Despite the lack of experimental data, the $CH_3H + {}^-CH_3$ couple and its comparison with the $^+NH_3H + NH_3$ and $HOH + {}^-OH$ couples will serve to analyze these questions.

The $CH_2{=}CH{-}CH_2H + {}^-CH_2{-}CH{=}CH_2$ couple will be used to observe and analyze the effect of charge localiza-tion−delocalization in a conjugated carbon acid, thus, putting the "principle of nonperfect synchronization" in a perspective that takes full account of the quantum character of proton transfer. It will also show how this effect originates in heavy-atom intramolecular reorganization that accompanies proton transfer.

Comparison of the $O_2NCH_2H + CH_2{=}NO_2^-$ and $CH_3H + {}^-CH_3$ couples will allow the examination of the changes elicited by the presence of a strong electron-withdrawing group and thus serve as the model example of a large series of experimental systems.

The next step is to combine all three preceding effects, taking the $O_2N{-}CH_2{=}CH{-}CH_2H + CH_2{=}CH{-}CH{=}NO_2^-$ system as an example.

The $^{+\bullet}H_2NCH_2H + {}^{\bullet}CH_2NH_2$ couple will provide a simple example of a radical cation, while the $^{+\bullet}H_2N{-}CH_2{=}CH{-}CH_2H + {}^{\bullet}CH_2{-}CH{=}CH_2{-}NH_2$ couple allows the examination of the role of the charge localization−delocalization energy in cation radical deprotonation.

In all of the cases, the analysis will produce a value of the protonation−deprotonation rate constant of the self-exchange reaction. In view of the approximate character of the estimate of several ingredients of the model used, of the approximations embodied in the model, and of the inaccuracy of quantum chemical calculations, the values thus found are expected to provide semiquantitative trends rather than accurate predictions. However, to check the validity of the trends observed with a density functional theory method used for all calculations (see the quantum chemical methodology section), QCISD calcula-tions have been performed on three couples of the list, namely, $CH_3H + {}^-CH_3$, $HOH + {}^-OH$, and $CH_2{=}CH{-}CH_2H + {}^-CH_2{-}CH{=}CH_2$, showing the same trends as those in the DFT calculations (see Supporting Information).

Modeling the Dynamics of Adiabatic and Nonadiabatic Proton Transfers.[21] Considering reaction Scheme 2, heavy-atom and proton coordinates are treated separately in the framework of the Born−Oppenheimer approximation, assuming that the proton adjusts itself instantaneously to heavy-atom reorganiza-tion. The reaction coordinate thus involves the latter factor rather than the coordinate defining the location of the proton, q (Scheme 2). More precisely, the reaction coordinate is subdi-vided into a coordinate, Q, that defines the relative position of the acid and the base (Scheme 2), a coordinate, Y, that indexes the intramolecular reorganization (changes in bond lengths and angles)[22a] of the A and B moieties, and a coordinate, X, a fictitious charge that indexes solvent reorganization in the Marcus way.[22b] The transition state is thus obtained as the energy minimum in the intersection of the reactant and product-free energy surfaces, $G_R(Q,X,Y)$ and $G_P(Q,X,Y)$:

$$G_R(Q,X,Y) = \frac{f_Q}{2}(Q - Q_R)^2 + \lambda_0(Q)X^2 + \lambda_i Y^2 \qquad (1)$$

$$G_P(Q,X,Y) = \frac{f_Q}{2}(Q - Q_P)^2 + \lambda_0(Q)(1 - X)^2 + \lambda_i(1 - Y)^2 + \Delta G^0 \qquad (2)$$

ΔG^0 is the standard free energy of the reaction, f_Q the force constant relative to the Q coordinate, and Q_R and Q_P the values of Q in the reactant and product systems, respectively. λ_i is the intramolecular reorganization energy. λ_i is practically indepen-dent of Q, whereas the solvent reorganization energy is a function of Q, given by[22b,c]

$$\lambda_0(Q) = \frac{e_0^2}{4\pi\epsilon_0}\left(\frac{1}{\epsilon_{op}} - \frac{1}{\epsilon_S}\right)\left(\frac{1}{2a_A} + \frac{1}{2a_B} - \frac{1}{Q}\right) \qquad (3)$$

where e_0 is the electron charge, ϵ_0 the vacuum permittivity, ϵ_{op} and ϵ_S the solvent optical and static dielectric constants, respectively, and a_A and a_B are radii of the sphere equivalent to A and B.

The two 4D surfaces intersect along the 3D surface defined by

$$\frac{f_Q}{2}(Q_P - Q_R)(2Q - Q_P - Q_R) + \lambda_0(Q)(2X - 1) +$$

$$\lambda_i(2Y - 1) = \Delta G^0 \quad (4)$$

At the transition state

$$\frac{\dfrac{\partial G_R}{\partial X}}{\dfrac{\partial G_P}{\partial X}} = \frac{\dfrac{\partial G_R}{\partial Y}}{\dfrac{\partial G_P}{\partial Y}} \quad \text{i.e., } X^{\ddagger} = Y^{\ddagger} \quad (5)$$

Thus from eqs 4 and 5

$$X^{\ddagger} = Y^{\ddagger} = \frac{1}{2}\left[1 + \frac{\Delta G^0 - \dfrac{f_Q}{2}(Q_P - Q_R)(2Q - Q_P - Q_R)}{\lambda_0(Q) + \lambda_i}\right]$$

The value of Q at the transition state, $Q^{\ddagger}$, is finally obtained from

$$\frac{dG_R^{\ddagger}}{dQ} = 0 \quad \text{with} \quad G_R^{\ddagger} = G_R(Q, X^{\ddagger}(Q), Y^{\ddagger}(Q))$$

i.e.

$$f_Q(Q - Q_R) + X^{\ddagger 2}\frac{\partial \lambda_0(Q)}{\partial Q} + 2\lambda_0(Q)X^{\ddagger}\frac{\partial X^{\ddagger}}{\partial Q} + 2\lambda_i Y^{\ddagger}\frac{\partial Y^{\ddagger}}{\partial Q} = 0$$

the activation free energy, $\Delta G^{\ddagger}$, being given by

$$\Delta G^{\ddagger} = G_R(Q^{\ddagger}, X^{\ddagger})$$

For self-exchange reactions, $Q_R = Q_P = Q_0$, and $\Delta G^0 = 0$. Thus, $X^{\ddagger} = Y^{\ddagger} = 1/2$, and

$$Q^{\ddagger 2}(Q^{\ddagger} - Q_0) + \frac{\dfrac{e_0^2}{4\pi\epsilon_0}\left(\dfrac{1}{\epsilon_{op}} - \dfrac{1}{\epsilon_S}\right)}{4f_Q} = 0 \quad (6)$$

The value of the force constant, f_Q, required to derive $Q^{\ddagger}$ from the preceding equation may be obtained from a quantum chemical calculation using a quadratic fitting of the variation of the energy with Q around the minimum, with all other variables being optimized. The minimum, characterized by $Q = Q_0$ and $X = Y = 0$, is a precursor complex. With self-exchange reactions, the successor complex also corresponds to Q_0 but with $X = Y = 1$. The next step is the computation of the proton-transfer profile in the geometrical configuration of the system at the transition state. For self-exchange reactions, this corresponds to $Y^{\ddagger} = 0.5$ and, therefore, to a symmetrical configuration midway between the precursor and successor complexes. The fact that the proton is transferred when the energy levels of the reactant and product match implies, in the case of a self-exchange reaction, that they have the same geometrical configuration. This configuration is thus obtained from the half-sum of the intramolecular coordinates of each of the two complexes after their optimization for $Q = Q^{\ddagger}$. The variation of the potential energy with the proton coordinate, q, for $Q = Q^{\ddagger}$ and for this particular geometrical configuration is finally computed, giving rise to a proton-transfer double-well profile of the type shown in Figure 1. In principle, the other hydrogen atoms present in the system (on the A and B moieties) should be allowed to move when the reacting proton is
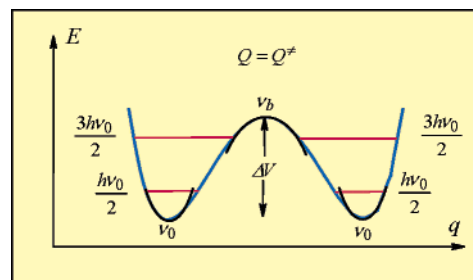
Figure 2. Tunneling in the nonadiabatic case.

transferred, and therefore their positions should be optimized together with the exchanging proton. However, as will be exemplified with the $CH_3H + {}^-CH_3$ system, the profiles obtained with all atoms fixed, including all hydrogens, except the transferring hydrogen, are practically the same. This simpler approach will therefore be followed throughout the following analysis.

When the proton barrier, ΔV, is small, as in the left-hand diagram of Figure 1, the zero-point energy stands above the barrier, thus giving rise to an adiabatic situation. In the nonadiabatic case, shown in the right-hand diagram of Figure 1, proton transfer involves tunneling through the barrier from the zero-point level and possibly a few higher vibrational levels.

In the adiabatic case, the rate constant is given by

$$k_{AD} = \nu \exp\left(-\frac{\Delta G^{\ddagger} + \Delta ZPE - C}{RT}\right)$$

where ΔZPE is the zero-point energy variation; C is the coupling constant between the two levels (the reactant and product-free energy surfaces at their intersection), and ν is a characteristic frequency appropriate for solvent fluctuations and intramolecular movements. C may be neglected in practice, leading to an expression of the rate constant that mostly depends on solvent reorganization and intramolecular reorganizations.

In the nonadiabatic case, the rate constant is the weighted sum of rate constants corresponding to the tunneling between pairs of vibrational levels of same height (Figure 2):[21e]

$$k_{NA} = \sum_{n=0}^{m} P_n k_{NA}^n \quad (7)$$

with each probability, P_n, being expressed as

$$P_n = \frac{\exp\left[-\dfrac{h\nu_0(n + 1/2)}{RT}\right]}{\displaystyle\sum_{n=0}^{m}\exp\left[-\dfrac{h\nu_0(n + 1/2)}{RT}\right]}$$

with m defined as $h\nu_0(m + 1/2) \leq \Delta V$ (ν_0 is the proton vibration frequency) and

$$k_{NA}^n = k_{NA}^{n,0}\sqrt{\frac{\pi}{2A_2}}\exp\left(-\frac{A_1^2}{2A_2}\right)$$

with

$$k_{NA}^{n,0} = \frac{4\pi^2}{h^2}C_n^2 \exp\left[2\frac{E_\beta}{h\nu_Q}\coth\left(\frac{h\nu_Q}{2k_BT}\right)\right]$$

Table 1. Parameters for the Calculation of the Rate Constants and Values of the Rate Constants[a]

acid	CH$_4$	H$_2$O	NH$_4^+$	CH$_2$=CH–CH$_3$	O$_2$NCH$_3$	$^+$H$_2$NCH$_3$	O$_2$N–CH$_2$=CH–CH$_3$	N$^+$H$_2$–CH$_2$=CH–CH$_3$
$f_Q^{b,c}$	0.546	5.925	5.000	0.625	1.026	1.200	0.740	0.558
$f_0^{b,d}$	13.7		5.33	15.0	10.47	6.62	21.50	12.42
$f_0^{b,d}$	13.7		5.33	15.0	10.47	6.62	21.50	12.42
$f_b^{b,d}$	6.3			6.0	6.12	4.10	10.32	7.44
$h\nu_Q^c$	0.0195	0.0556	0.054	0.021	0.027	0.030	0.023	0.020
$h\nu_0^d$	0.239		0.149	0.250	0.210	0.166	0.300	0.228
$h\nu_b^d$	0.162			0.158	0.160	0.131	0.207	0.176
Q_0^c	3.413	2.47	2.677	3.420	3.149	3.117	3.535	3.418
$Q^{\ddagger e}$	3.239	2.442	2.648	3.270	3.044	3.027	3.420	3.246
ΔV^f	0.406	0.0	0.0125	0.406	0.189	0.112	0.760	0.40
$\lambda_0(Q^\ddagger)^g$	0.765	0.362	0.489	0.777	0.686	0.678	0.830	0.768
λ_i	0.140	0.0	0.0	0.688	0.360	0.152	1.440	0.870
E_β^h	0.314	0.235	0.269	0.314	0.314	0.314	0.314	0.314
$\log k^i$	3.3	9.95	9.4	0.9	5.6	7.1	−5.9	0.3

[a] Force constants are in eV Å^{-2}, energies in eV, and distances in Å. [b] With $f = (2\pi\mu\nu)^2$. [c] With ν_Q from the potential energy vs Q diagrams in the Supporting Information; $\mu = 6$ amu, except for NH$_4^+$, where $\mu = 7$ amu, and for H$_2$O, where $\mu = 8$ amu. [d] With ν_0 and ν_b from the potential energy vs q diagrams in Figures 3, 5, and 7−10 (as depicted in Figure 2); $\mu = 1$ amu. [e] From eq 4, taking $(e_0^2/4\pi\epsilon_0)(1/\epsilon_{op} - 1/\epsilon_S) = 4$, as derived from experimental values found in the application of Hush−Marcus theory to homogeneous self-exchange reaction in DMF,[23a] rather than direct application of the Born-like Marcus formula expected to overestimate solvation energies, as discussed in ref 20b. [f] From the potential energy vs q diagrams in Figures 3, 5, and 7−10 (as depicted in Figure 2). [g] From eq 3, taking $a_R = a_P = 2$ Å. [h] From eq 8, taking $\beta = 30$ Å^{-1}, as indicated in ref 16 or 18d, and checked here at the occasion of several calculations involving potential energy vs Q profiles. [i] Bimolecular rate constant in M^{-1} s^{-1} derived according to the procedure described in the text with $Z/\nu = 0.05$ M^{-1}.

ν_Q corresponds to the force constant, f_Q, defined earlier. The various constants thus introduced are defined as follows.

$$C_n = \frac{h\nu_0}{2}\exp\left\{-\frac{\pi}{h\nu_b}\left[\Delta V - h\nu_0\left(\frac{1}{2} + n\right)\right]\right\} = C_0 \exp[-\beta(Q - Q_0)]$$

where the distance attenuation constant, β, is defined as

$$\beta = -\frac{\pi}{h\nu_b}\frac{\partial\left[\Delta V - h\nu_0\left(\frac{1}{2} + n\right)\right]}{\partial Q}$$

$$A_1 = \frac{2\pi}{h}(\Delta G^0 + \lambda_0 + \lambda_i + \lambda_Q + E_\beta)$$

$$A_2 = \frac{8\pi^2 k_B T}{h^2}\left[\lambda_0 + \lambda_i + (\lambda_Q + E_\beta)\frac{h\nu_Q}{2k_B T}\coth\left(\frac{h\nu_Q}{2k_B T}\right) + \frac{Q_P - Q_R}{|Q_P - Q_R|}\left(\frac{h\nu_Q}{k_B T}\right)\sqrt{\lambda_Q E_\beta}\right]$$

ν_b is the frequency corresponding to a parabolic approximation of the barrier top (Figure 2).

$$E_\beta = \frac{h^2\beta^2}{8\pi^2 m_Q} \quad (m_Q \text{ is the A−B reduced mass}) \qquad (8)$$

$$\lambda_Q = \frac{f_Q}{2}(Q_P - Q_R)^2$$

In the case of a self-exchange reaction, $\Delta G^0 = 0$ and $\lambda_Q = 0$, the expressions of A_1 and A_2 reduce to

$$A_1 = \frac{2\pi}{h}(\lambda_0 + \lambda_i + E_\beta)$$

$$A_2 = \frac{8\pi^2 k_B T}{h^2}\left[\lambda_0 + \lambda_i + E_\beta\frac{h\nu_Q}{2k_B T}\coth\left(\frac{h\nu_Q}{2k_B T}\right)\right] \cong \frac{8\pi^2 k_B T}{h^2}(\lambda_0 + \lambda_i + E_\beta)$$

since at room temperature, $h\nu_Q \ll k_B T$. It follows that

$$k_{NA}^n = k_{NA}^{n,0}\sqrt{\frac{h^2}{16\pi k_B T(\lambda_0 + \lambda_i + E_\beta)}}\exp\left(-\frac{\lambda_0 + \lambda_i + E_\beta}{4k_B T}\right) \qquad (9)$$

This procedure leads to a monomolecular rate constant, k_{NA}, that can be converted into the corresponding bimolecular rate constant in which the experimental data are cast, according to the following relation: $k_{NA}^b = (Z/\nu)k_{NA}$. (Z is the bimolecular collision frequency, and ν is the characteristic frequency appropriate for solvent fluctuations and intramolecular movements.)

Applications to Typical Self-Exchange Reactions. We now apply the preceding equation to the eight self-exchange reactions listed in the Introduction. We start with the determination of Q_0 and f_Q by deriving these values from the quantum chemical calculation of the potential energy versus Q diagrams (see Supporting Information) that leads to the values listed in Table 1. The value of Q for the transition state from eq 6 and $\lambda_0(Q^\ddagger)$ is then obtained from eq 3. Geometrical optimizations of the system for $Q = Q^\ddagger$, with the proton located on one base and then on the other base, lead to two complexes of identical energy. An average of their geometrical intramolecular coordinates gives the geometrical configuration at the transition state. The potential energy versus q profile (Figure 2) is then computed with this fixed configuration. The results are displayed in Figures 3, 5, and 7−10. Assuming a quadratic variation for the internal reorganization (eqs 1 and 2), we may deduce the internal reorganization energy, λ_i, from the difference between the energies of the system at $Q = Q^\ddagger$ when $Y = 0$ (E_{pc}) and when $Y = 0.5$ ($E^\ddagger$)

$$\lambda_i = 4(E^\ddagger - E_{pc})$$

The remaining ingredients required to obtain the rate constants are listed in Table 1.

The rate constant is finally computed according to the case, adiabatic for the H$_2$O/OH$^-$ and $^+$NH$_4$/NH$_3$ couples and nonadiabatic for all carbon acids; the intermediate constants introduced in the series of equations given above for this case are derived from the parameters listed in Table 1. As can be shown in Figure 3 for the CH$_3$H + $^-$CH$_3$ system, computation of the
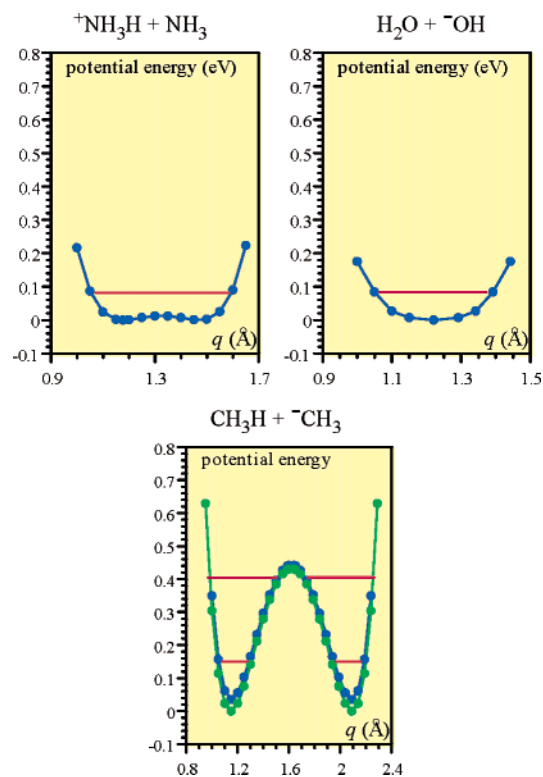
Figure 3. Potential energy versus q profiles at $Q = Q^{\ddagger}$. Comparison between a carbon acid, CH$_4$, and two Eigen acids, NH$_3$ and H$_2$O. For CH$_4$, two profiles are represented: with fixed hydrogen atoms (other than the transferring proton) (blue dots) and with optimized hydrogen atoms (other than the transferring proton) (green dots).

Figure 4. Gas-phase potential energy versus Q profiles. Comparison between a carbon acid, CH$_4$ (green dots), and two Eigen acids, NH$_3$ (red dots) and H$_2$O (blue dots).

Figure 5. Potential energy versus q profiles at $Q = Q^{\ddagger}$. Nonperfect synchronization effect: the propene/allyl carbanion couple compared to the methane/methyl carbanion couple.

energy profile as a function of q, with or without fixed hydrogen atoms, has no significant effect on the proton barrier and therefore on the intramolecular reorganization energy.

Note also that for the purpose of simplicity, we have taken a common value for the solvation radius in eq 3, an approximation that matches the semiquantitative approach that we follow.

Discussion

The difference in behavior between CH$_4$ on one hand and NH$_3$ and H$_2$O on the other (Figure 3) is striking; the proton barrier with the first acid is so much higher than that with the two others that proton transfer between CH$_4$ and CH$_3^-$ belongs to the nonadiabatic category, while the $^+$NH$_4$/NH$_3$ and H$_2$O/OH$^-$ couples fall in the adiabatic case, as already pointed out by several studies.[1e,15] With NH$_3$ and H$_2$O, the dynamics of proton transfer therefore does not depend on the proton barrier but rather on heavy-atom reorganization, essentially solvent reorganization. The situation is similar to what happens with outersphere electron transfer. In the case of CH$_4$, too, heavy-atom reorganization interferes under the form of an exponential term, but the proton barrier interferes jointly, albeit, in the pre-exponential term, as a result of tunneling through the barrier between two pairs of vibrational states. The way in which the proton barrier governs the dynamics of the reaction is thus quite different from the classical transition-state theory relationship:

$$k = Z \exp\left(-\frac{\Delta G^{\ddagger}}{k_{\mathrm{B}}T}\right) \quad (10)$$

In addition, the gas-phase barriers, quantum chemically calculated in the usual way, do not correspond to the same value
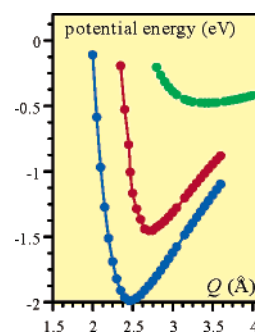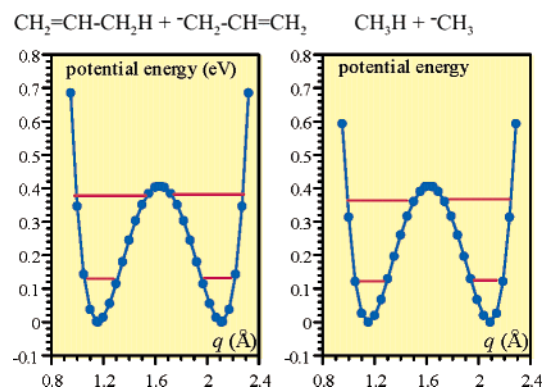
of the coordinate $Q^{\ddagger}$ that is used in the present analysis. It remains nevertheless that, qualitatively speaking, the higher the proton barrier, the slower the reactions, even if eqs 7 and 9 have to be used instead of eq 10.

The main factor that makes the proton barrier so small with NH$_3$ and H$_2$O is the fact that the value of Q at the transition state (ninth row in Table 1) is much smaller than that with CH$_4$ (Figure 4), which is in agreement with previous work.[15,19,20a]

The reason for this difference is that the dipolar character of the N−H and O−H bonds is much larger than that of the C−H bond, thus decreasing Q_0 because of a stronger interaction with the negative charge on the other member of the self-exchange couple. In other words, this difference in behavior is related to more ionic character of the bond in the first two cases than with CH$_4$ (A$^-$ H$^+$ $^-$A vs A⋯H $^-$A and A$^-$ H⋯A), which is in line with the stronger electron affinity of NH$_3^{+\bullet}$ and OH$^{\bullet}$ as compared to that of CH$_3^{\bullet}$. At this stage, we may thus answer the title question by stating that the reason that proton transfer at carbon is slow is that carbon stands in the middle of the periodic table.

We now address the question of imbalanced transition states with the example of propene (Figure 5). The values of Q at the transition state (Table 1) are practically the same for propene and methane, and the proton activation barrier is also practically the same. The smaller value of the rate constant corresponds, in fact, to a substantially larger value of the intramolecular reorganization energy, λ_i (0.688 eV instead of 0.140 for methane). For the reasons detailed below, this large value of λ_i reflects the energy of the charge localization−
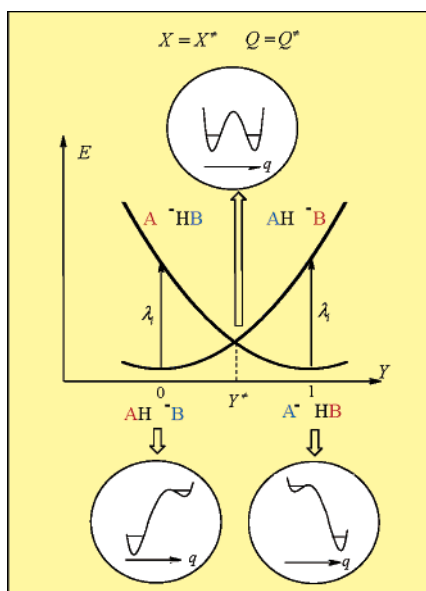
Figure 6. Effect of intramolecular reorganization. Potential energy versus Y profiles for $Q = Q^{\ddagger}$ and $X = X^{\ddagger}$. Red letters: ground-state configuration in the acid. Blue letters: ground-state configuration in the base. Insets: potential energy versus q profiles for $Y = 0$, $Y = Y^{\ddagger}$, and $Y = 1$.

delocalization process required for proton transfer to occur. Within the framework of the Born–Oppenheimer treatment of proton transfer, it corresponds to the notion of imbalanced transition states and nonperfect synchronization in previous treatments.

Considering only the Y coordinate at $Q = Q^{\ddagger}$ and $X = X^{\ddagger}$, the heavy-atom system is described by two diabatic states intersecting at $Y = Y^{\ddagger}$, as shown in Figure 6. Thus, as far intramolecular reorganization is concerned, the Franck–Condon term of proton transfer is governed by the intramolecular reorganization energy, λ_i, and by the degree of coupling between both states (fluctuation splitting). Since we are dealing with carbon acids, the coupling is weak owing to the large separation between the two proton-transferring carbons. In the framework of the quadratic model delineated by eqs 1 and 2, the intramolecular activation barrier is one-fourth of λ_i. For the following reasons, substantial intramolecular reorganization energy is expected with systems involving a delocalized base as the propene/alkyl anion couple. As shown in Figure 6, the internal reorganization energy corresponds to the energy difference of the reactant and product states at $Y = 0$. There, using the notations in Figure 6, in the reactant state, the B moiety is a delocalized allyl anion that can be described by two resonant forms, $CH_2\!=\!CH\!-\!CH_2^- \leftrightarrow {}^-CH_2\!-\!CH\!=\!CH_2$, while the A moiety corresponds to a localized double bond in propene, $CH_2\!=\!CH\!-\!CH_3$. In the product state, still for $Y = 0$, the geometrical structures are unchanged, except that the proton has been transferred leading to a localized base, A^-, described by a single form, $CH_2\!=\!CH\!-\!CH_2^-$, while the propene HB has now to be described by two limiting forms, $CH_2\!=\!CH\!-\!CH_2H \leftrightarrow {}^-CH_2\!-\!CH\!=\!CH_2H^+$. It thus appears that the more delocalized the base, the larger the intramolecular reorganization, thus explaining the difference in rate constant observed between propene and methane. Through this analysis, the Y coordinate can be viewed as an index of charge localization (or delocalization). The notion of an imbalanced transition state, as defined
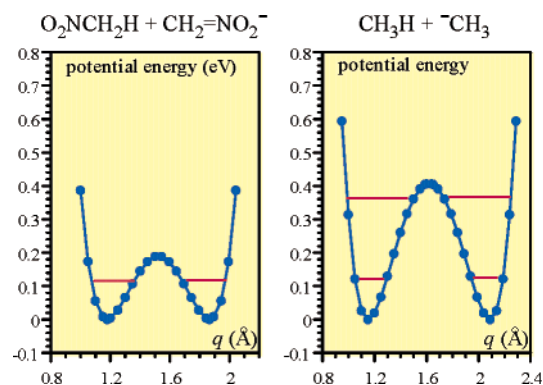

Figure 7. Potential energy versus q profiles at $Q = Q^{\ddagger}$. Nitromethane compared to methane.
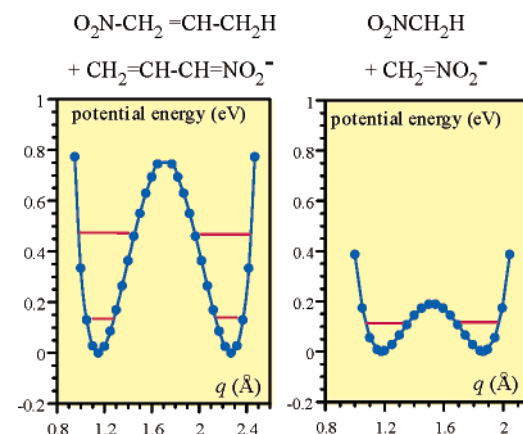

Figure 8. Potential energy versus q profiles at $Q = Q^{\ddagger}$. Nitromethane compared to nitropropene.

in Scheme 1, should thus be placed within the context of charge localization–delocalization heavy-atom intramolecular reorganization rather than of synchronization (or lack of) between charge delocalization and proton transfer.

With nitromethane (Figure 7), we observe the combination of two effects. One reflects the fact that the value of $Q^{\ddagger}$ is smaller than with methane (Table 1), resulting in a smaller proton-transfer barrier, in line with an increased contribution of the ionic state due to higher electron affinity of the radical. This decrease of the barrier is however not as important as that with NH_3 and H_2O. It is not sufficient to achieve adiabatic conditions just to make tunneling easier.

A second effect, going in the opposite direction, results from the charge localization–delocalization reorganization. This effect manifests itself at the level of the internal reorganization energy, λ_i, which is higher with nitromethane than with methane. This second effect is however small, smaller than with propene.

A further example of the importance of charge localization–delocalization reorganization upon proton transfer is found when a double bond is inserted between the carbon and nitrogen atom of nitromethane (Table 1), as revealed by a large increase of the intramolecular reorganization energy as compared to nitromethane. The reaction is additionally slowed by a significant augmentation of the proton-transfer barrier due to a higher value of $Q^{\ddagger}$ (Figure 8), leading to a substantial increase of the proton-transfer barrier. This difference with the nitromethane case may be explained as follows. The electron affinity of the nitroallyl radical is not expected to be drastically different from that of
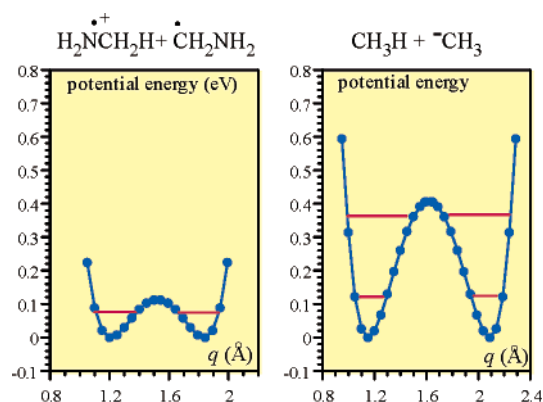
Figure 9. Potential energy versus q profiles at $Q = Q^{\ddagger}$. Cation radical of methylamine compared to methane.

Figure 10. Potential energy versus q profiles at $Q = Q^{\ddagger}$. Comparison between the cation radicals of aminopropene and methylamine.

the nitromethyl radical, leading to similar relative contributions of the ionic state. The negative charge in the carbanion, mostly located on the terminal NO_2 group in both cases, is however more distant from the acid molecule, leading to a weaker interaction in the first case than in the second.

Addition of the two effects leads to a considerable decrease of the self-exchange rate constant (Table 1). The rate constant thus found for nitropropene may seem unrealistically low as compared to the value found for the standard rate constant for a similar carbon acid, namely, *p*-nitrotoluene.[1b] It should however be taken into account that the standard rate constant pertains to the reaction of the carbon acid with the base of a "normal" acid−base couple that has the same pK_a value as the carbon acid (zero driving force). The self-exchange reactions we are dealing with are also endowed with a zero driving force, but involve, in contrast, a carbon acid and its conjugate base. Since Eigen couples are fast, we expect the self-exchange reaction to be much slower than a zero driving force reaction involving a normal acid−base couple. This remark also applies to the other carbon acids under examination even if their self-exchange rate constant is not as small.

The simplest cation radical that we have considered, the cation radical of methylamine, shows a quite significant increase of the rate constant (Table 1) as compared to that of methane. This results again from a decrease of the proton-transfer barrier concomitant with a substantial decrease of $Q^{\ddagger}$ (Figure 9). In this case, there is a strong contribution of the ionic state, $^{\bullet}H_2NCH_2$ H^+, relative to the homolytic state owing to the high electronic affinity of $^+H_2NCH_2\cdots H$ and $^+H_2N=CH_2H$, leading to a strong interaction with the zwitterionic neutral radical that serves as the base.

The presence of a cation radical substituent thus has an effect similar to that of an electron-withdrawing substituent, such as NO_2.

The comparison of internal reorganization energies between the cation radicals of dimethylamine and aminopropene (Table 1) provides a further example of the importance of charge localization−delocalization reorganization upon proton transfer in conjugated acids, as well as effect of $Q^{\ddagger}$ (Figure 10).

Concluding Remarks

The self-exchange deprotonation of all carbon acids investigated fall into the nonadiabatic category, as opposed to the two typical Eigen acids, water and ammonia. In the former case,
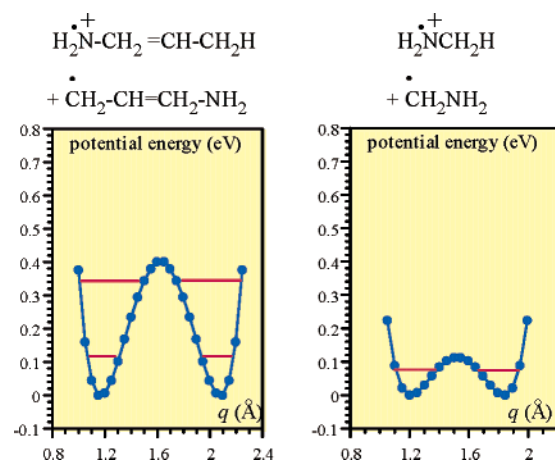
in addition to solvent and intramolecular reorganization, the reaction dynamics is thus governed at the level of the pre-exponential factor by the characteristics of the barrier through which the proton tunnels.

The resulting intrinsic slowness of a nonactivated acid, like methane, is related to the fact that the distance between the carbon centers in the transition state is larger than between the nitrogen or oxygen atoms in ammonia and water, respectively. This difference is itself a consequence of the less-polar character of the C−H bond as compared to that of the N−H and O−H bonds in ammonia and water. A rational basis is thus given to the intuitive notion that intrinsic slowness of carbon acids is related to the fact that carbon stands in the middle of the periodic table.

The increase of polarity of the carbon−hydrogen bond caused by the presence of an electron-withdrawing substituent, such as a nitro group, is likewise the reason that the proton barrier decreases. An increase of the pre-exponential factor ensues, while the reaction remains nonadiabatic.

The presence of a cation radical substituent has a similar effect, for similar reasons, as an electron-withdrawing substituent.

Intramolecular reorganization appears as an important factor in conjugated acids that are presumed to give rise to imbalanced transition states with nonactivated acids, such as propene, as well as with electron-withdrawal-activated acids, such as nitropropene or the cation radical of aminopropene. It corresponds to the charge localization−delocalization energy required for proton transfer to occur. The notion of an imbalanced transition state should thus be placed within the context of charge localization−delocalization heavy-atom intramolecular reorganization rather than of synchronization (or lack of) between charge delocalization and proton transfer.

Quantum Chemical Calculation Methodology. All of the calculations were performed with the Gaussian 98 series of programs.[24] The DFT method (B3LYP) was used. An unre-

(21) (a) We used, as the general framework, the Lee−Borgis−Hynes theory of proton transfer,[21b−e] with a slight change concerning the way in which solvent reorganization is taken into account and with the inclusion of intramolecular reorganization through the Y variable. (b) Borgis, D.; Lee, S.; Hynes, J. T. *Chem. Phys. Lett.* **1989**, *162*, 19. (c) Borgis, D.; Hynes, J. T. *J. Chem. Phys.* **1991**, *94*, 3619. (d) Borgis, D.; Hynes, J. T. *Chem. Phys.* **1993**, *170*, 315. (e) Lee, S.; Hynes, J. T. *J. Chim. Phys.* **1996**, *93*, 1783.

stricted version of the theory (UB3LYP) was used for systems involving open-shell structures. The 6-31G* basis set was used. Minimum energy structures were fully optimized with a geometrical constraint forcing the hydrogen atom transferred and both atoms bonded to it to be collinear. QCISD calculations have been performed on three systems, namely, $CH_3H + {}^-CH_3$, $HOH + {}^-OH$, and $CH_2{=}CH{-}CH_2H + {}^-CH_2{-}CH{=}CH_2$.

Supporting Information Available: Potential energy versus Q profiles and all QCISD results. This material is available free of charge via the Internet at http://pubs.acs.org.

JA046467H

(22) (a) Marcus, R. A. *Discuss. Faraday Soc.* **1960**, *29*, 21. (b) Marcus, R. A. Theory and applications of electron transfers at electrodes and in solution. In *Special Topics in Electrochemistry*; Rock, P. A., Ed.; Elsevier: New York, 1977; pp 161−179. (c) This equation, originally derived for electron-transfer reactions, can be applied in the present case insofar as it is based on electrostatic relationships applied to charge distributions approximated by spheres.

(23) (a) Kojima, H.; Bard, A. J. *J. Am. Chem. Soc.* **1975**, *77*, 5317. (b) Andrieux, C. P.; Savéant, J.-M.; Tardy, C. *J. Am. Chem. Soc.* **1998**, *120*, 4167.

(24) Frisch, M. J.; Trucks, G. W.; Schlegel, H. B.; Scuseria, G. E.; Robb, M. A.; Cheeseman, J. R.; Zakrzewski, V. G.; Montgomery, J. A., Jr.; Stratmann, R. E.; Burant, J. C.; Dapprich, S.; Millam, J. M.; Daniels, A. D.; Kudin, K. N.; Strain, M. C.; Farkas, O.; Tomasi, J.; Barone, V.; Cossi, M.; Cammi, R.; Mennucci, B.; Pomelli, C.; Adamo, C.; Clifford, S.; Ochterski, J.; Petersson, G. A.; Ayala, P. Y.; Cui, Q.; Morokuma, K.; Malick, D. K.; Rabuck, A. D.; Raghavachari, K.; Foresman, J. B.; Cioslowski, J.; Ortiz, J. V.; Stefanov, B. B.; Liu, G.; Liashenko, A.; Piskorz, P.; Komaromi, I.; Gomperts, R.; Martin, R. L.; Fox, D. J.; Keith, T.; Al-Laham, M. A.; Peng, C. Y.; Nanayakkara, A.; Gonzalez, C.; Challacombe, M.; Gill, P. M. W.; Johnson, B. G.; Chen, W.; Wong, M. W.; Andres, J. L.; Head-Gordon, M.; Replogle, E. S.; Pople, J. A. *Gaussian 98*; Gaussian, Inc.: Pittsburgh, PA, 1998.